Multi-scale Interaction of Flow and the Artery Wall

, I. HALLIDAY [1,*], S. V. LISHCHUK [1]M. A. ATHERTON [2], C. M. CARE [1], M. W. COLLINS [2], D. EVANS [3], P. C. EVANS [4], D. R. HOSE [3], A. W. KHIR [2], R. KRAMS [5], P. V. LAWFORD [3], V. RIDGER [6], Y. VENTIKOS [7], D. C.WALKER [8], P. N. WATTON [7]

* Corresponding author: Tel.: ++44 (0)114 2253045; Fax: ++44 (0)114 22530**; Email: i.halliday@shu.ac.uk

1 Materials and Engineering Institute, Sheffield Hallam University, Sheffield UK

2 School of Engineering and Design, Brunel University, London UK

3 Academic Unit Medical Physics and Clinical Engineering, University of Sheffield, Sheffield UK

4 BHF Cardiovascular Sciences Unit, National Heart and Lung Institute, Imperial College, London UK

5 Department of Bioengineering, Imperial College London, London UK

6 Cardiovascular Research Unit, University of Sheffield, Sheffield UK

7 Institute of Biomedical Engineering, Department of Engineering Science, University of Oxford, Oxford UK

8 Department of Computer Science, University of Sheffield, Sheffield UK

Abstract We discuss, from the perspective of basic science, the physical and biological processes which underlie atherosclerotic (plaque) initiation at the vascular endothelium, identifying their widely separated spatial and temporal scales which participate. We draw on current, related models of vessel wall evolution, paying particular attention to the role of flow, and proceed to propose, then validate (in practical, qualitative terms, at least) a multiply coupled, multi-scale modeling strategy, which, eventually, aims at a quantitative, patient-specific understanding of the coupling between the flow and the endothelial state.

Keywords: Multi-scale, Microcirculation,

1 Introduction Atherosclerosis has the highest mortality in the western world. Although it is known to be lipid-driven, inflammation and blood flow, have generated recent interest as alternative or complementary explanations for the formation atherosclerotic lesions (plaques) (1,2). The role of flow, long evident in the observation that plaques occur near arterial side branches, bifurcations, or bends of low curvature (where flow rates and shear are low, disturbed or oscillatory) is coupled to other processes by activation of the vascular endothelium, which, when healthy, inhibits leukocyte adhesion, platelet aggregation and exhibits anti-inflammatory, anti-proliferative and anti-oxidant characteristics. A dysfunctional endothelium is a key mediator in the pathogenesis of arterial disease (3,4). As this article proceeds, it will become clear that the physics and biology of these mechanisms is located on widely separated spatial and temporal scales- a fact which calls for a particular approach to the problem of developing a quantitative model In this brief article, then, we describe, and contextualize our recent progress towards a complex, multi-scale, *in silico* model of plaque initiation, which originates from, and is closed by, basic science. Section 2 and the references therein provide background to the participating biological and physical mechanisms, whist emphasizing their spatial-temporal locations. Sections 3 and 4 discuss the recognized problems associated with the task of coupling together such disparate scales and advances our particular solution, of multi-scale modeling to achieve correct, self-consistent coupling of the state of the endothelium with flow. In section 5 we present preliminary results and in section 6, our conclusions and intentions for future work.

2 Background The healthy arterial wall (Figure 1) is comprised of endothelial cells (ECs), smooth muscle cells and fibroblasts. The vascular endothelium, which regulates vascular inflammation, consists of an EC monolayer on a collagen basement membrane: it serves to regulate the capture and subsequent infiltration of inflammatory cells (eg leukocytes) into the underlying tissue. Multi-scale processes couple its function, directly and indirectly, (eg. by chemical convection-

diffusion) to plaque formation.

Flow affects endothelial expression of several adhesion proteins which govern capture and rolling of leukocytes on the endothelial surface, from the bloodstream, and it also distributes leukocytes and erythrocytes within the lumen (margination) (5).Furthermore, wall shear stress (WSS) influences EC physiology, assisting leukocyte ingress (see below) (5). During leukocyte attachment, similarly structured P- or L-type selectins (on leukocyte microvilli and ECs) mediate capture, in a process which may be modeled on the surface rolling of an incompressible drop with regulated wetting (5,6). Longer periods of endothelial stimulation increase adhesion factor density, increase protein-protein interaction, so slowing rolling velocity, under the influence of E-selectin (7) exposing a leukocyte to endothelial chemoattractants, resulting in firm adhesion.

Flow has another direct role. The structural arrangement and morphology of ECs is mechanically influenced. In turn, local wall topography influences local shear stress: an alignment of ECs with flow direction reduces the maximum shear stress by 50% (10) in a two-way coupling. Increased WSS increases stiffness and alters the properties of ECs (9): *in vitro*, ECs elongate, changing from a polygonal 'cobblestone' morphology to flattened, elongated ovoids (Figures 2a, 2b), the degree of elongation correlating with the magnitude of the shear stress (10-13) (note, shear stress *type* too is relevant: under oscillatory shear, cultured cells retain a polygonal shape (11)) and *in vivo*, ECs have been shown to orientate to the predominant local flow direction (14), perpendicular to the direction of cyclic stretch (15,16). Such observed behavior should, of course, emerge from a correct and self-consistent model coupling the endothelial state with flow. Tarbell et.al. suggested that stretch and direction of streamlines are perpendicular to each other in straight vessel segments, thereby amplifying each other. Near side-branches and in disease, the orthogonality of both biomechanical factors is lost and endothelial homoeostasis is affected, leading to a pro-atherogenic environment.

In normal arteries, WSS ranges between 10 and 70 dynes/cm^2 (1-7 Pa), a mean positive value characterizing the optimal state. In the latter, ECs align with flow, integrin distribution is reorganized, improving EC adhesion, and anti-thrombic and vasoactive agents (nitric oxide, endothelium-derived hyperpolarizing factor, prostacyclin and endothelin) are produced (17,18) to act on the vascular smooth muscle cells, which regulate the diameter of the vessel and so control local blood flow rate (19). Local regulation of vessel diameter helps to maintain WSS within the normal range. As we have noted, higher and lower values of WSS and of oscillating shear index (OSI) are found at specific sites in the circulation, in association with changes in geometry (eg. an anastomosis, stenosis or bifurcation,) with the lowest values being found where flow becomes unstable, with associated flow separation, recirculation zones or stagnant regions. Specific levels of shear stress are believed to result in increased levels of the biomarkers, discussed above, associated with inflammatory pathways. Historically, high WSS is considered atheroprotective (20), whereas low WSS is associated with atherogenesis (3). Several studies suggest that oscillatory shear is also detrimental; for example, Ku *et al* (21), correlate atherosclerotic plaque location with areas of low and oscillating WSS in the human carotid bifurcation. An additional level of complexity is demonstrated by the results of *in vitro* studies indicating that ECs can sense temporal and spatial gradients of WSS (22-24).

In the substantial literature on the influence of shear stress on ECs, most data has been obtained from *in vitro* experiment using rigid flow chambers and well-characterised flows, when WSS can be calculated with a reasonable level of confidence. *In vivo*, the situation is more complex and the WSS values obtained represent a mean over a considerable area of the vessel wall and, hence, are not descriptive of individual cells. This approximation may be reasonable, for there is evidence of significant interaction and intercellular signaling between ECs (25), but the length-scale of any response

homogenization remains unclear. Additional questions arise when one considers the meso-scale and micro-scale constitution of blood.

Steady haemodynamic flow approximates the real experience of ECs, which must view the flow of the blood as motion of a high volume fraction particle suspension, comprised (at its simplest), of erythrocytes and incompressible plasma. On this view, necessarily *unsteady* stresses imparted, on the endothelium, have contributions from fluid stresses *and* particle impacts and have a spatial/temporal structure neglected by the continuum haemodynamic approximation. The unstudied, statistical properties of such "real" stress distributions will depend, *inter alia*, upon correlations with the macro-geometry and local micro-geometry (instantaneous conformation of ECs). They will also depend on the microscopic surface structure of the erythrocytes.

Boundary conditions which describe advected erythrocytes' encounter with ECs are not necessarily no-slip, Dirichlet conditions. Instead, Navier-type conditions, depending in turn, upon the microscopic properties of the membrane-bound macromolecular coating, found on the ECs' luminal surface, the glycocalyx, must be considered. Comprising sulphated proteoglycans, hyaluronan and glycoproteins, the glycocalyx has a net negative charge and it binds blood-born molecules such as plasma proteins, enzymes cytokines, water and other molecules with cationic sites in a layer ~500nm thick (26). Interestingly, the thickness of this layer is reduced at sites where atherosclerosis is initiated.

The physics, biology and the scales of the coupled processes outlined in this section urge a multi-scale approach to a quantitative understanding of endothelial behavior, based on interfacing a range of appropriately adapted, two-way coupled computational strategies. We will discuss our approach in section 4: first we review that current work which provides its basis.

3 Coupling vessel evolution to flow Xu and Collins (27) showed that, to be meaningful clinically, traditional CFD, based upon discretization of the Navier-Stokes and continuity equations and an appropriate constitutive equation for blood (approximated as a continuum) should have the potential to address: a] the time-dependent pulsatility of blood flow, b] the non-Newtonian character of blood (ie the non-linear relationship between viscosity and shear stress), c] the 3D geometry of the arterial system, and d] its time-dependence due to the distensibility of the arterial wall. Several data sources are essential to the development of a closed computational model; a description of the boundary conditions, a description of blood viscosity and appropriate sets of validation data, against which key features of the model's output might be tested. *In vitro* experiments by Moravec and Liepsch (28) were used in this capacity (29), later *in vivo* canine bifurcation data (30) were added before the model was extended to accept clinical Magnetic Resonance (MR) data for inlet boundary conditions (31). Finally, a number of alternative fluid-structure-interaction (FSI) models were successfully validated using Womersley's data (32). CFD codes have now been combined with solid mechanics codes to give immediate FSI capability but, for cardiovascular vessels, there remains a paucity of data on the constraints on vessel wall motion *in vivo*. One solution is to use time series image data to describe wall motion. In a very recent study characterising the haemodynamics of the human superior mesenteric artery (SMA), a fully transient, CFD model was constructed of a segment of the abdominal aorta and SMA. The geometry was based on dynamic MR imaging data and boundary conditions (flow), were determined from phase contrast MR velocity measurements (34). The abdominal aorta, was shown to be a principal site for the development of atherosclerotic lesions (33) as are the immediate proximal (coeliac) and distal (renal) branches. (see the AneurIST project (www.aneurIST.org)). The resulting OSI map for the model is shown in Figure 3a. OSI is, in general, lower in the SMA than in the aorta. The only area of high OSI in the SMA is at the root of the vessel as it leaves the aorta. This correlates with clinical observations for

atheroma. Figure 3b illustrates the time varying WSS for two areas of the vessel wall exposed to a high or low level of OSI. .

Tissue remodeling and endothelium signaling have been incorporated into coupled simulations. The evolution (inception, growth and rupture) of cerebral aneurysms provides an illustrative example of a class of models which have applications to disease evolution, as well as to the evaluation of competing theories. Aneurysm risk evaluation involves factors of genetics and vasculature geometry as well as mechanical properties of the tissue and blood flow details. The first modeling stage is to estimate the haemodynamic loads (pressure and WSS) acting on the aneurysm and parent artery using a finite volume technique. The distribution of WSS on the inner surface of the aneurysm is computed and used to model a hypothetical endothelial response which subsequently signals the smooth muscle cells and fibroblasts and leads to a remodeling and growth/atrophy of the elastin and collagen in the arterial wall. This results in changes in the mechanical properties of the aneurysm and the geometry adapts to maintain mechanical equilibrium; a finite element method is used to solve the updated deformation field. The new geometry changes the haemodynamics and, the WSS distribution and an updated flow field is solved, the computational cycle being repeated until the aneurysm stabilises in size or until the loads imposed exceed the load-bearing capacity of the wall leading to rupture.

Such integrative models can be used to relate growth/remodeling of the arterial wall to the haemodynamic stimuli acting on ECs. For instance, the magnitude of the spatial WSS gradient (WSSG) has been proposed as one possible haemodynamic parameter which is correlated with regions of pathological remodeling (35). As an aneurysm adapts the WSSG spatial distribution (see Figure 4) acting on the endothelium will change substantially: subsequent effects on tissue remodeling is of critical importance.

These models' uncertainties are, ideally, removed by resolving the cellular-scale (with proper account of the issues raised in section 2). Here, such a step requires one to depict interactions between ECs and flow and demands explicit representation of blood cells and plasma. CFD-based haemodynamics treats blood flow as a flow of continuous fluid and the vascular endothelium as the relevant, geoemetrically complex, velocity boundary condition. In reality, a local endothelial state emerges from encounters between individual (but interacting) ECs in a Newtonian plasma advecting discrete particles whose encounter with individual ECs is determined by local geometry, flow rate and cell concentration.

4 Multi-Scale Models of Vessel Evolution. Work such as that outlined in the previous section couples independent, essentially macroscale models. There are however, situations which require the simultaneous use of microscopic and mesoscopic models.

Investigations of the interaction of intravascular devices with the arterial wall, specifically; the Intra Aortic Balloon Pump (IABP) and vascular stent demonstrate a need to address smaller scales in general and the endothelium (and possibly the glycocalyx) in particular. An Intra Aortic Balloon Pump (IABP) is used to support a failing heart and is usually inserted in the abdominal aorta, via the iliac artery, then inflated (during diastole) and deflated (during systole) every-, every other- or every second cardiac cycle, aiming to increase coronary flow and reduce left ventricular after-load. Inevitably, the balloon contacts the inner wall of the aorta with every inflation/deflation cycle, which is believed to lead to balloon rupture. As the balloon approaches the endothelium, a volume of blood is displaced proximally and distally, generating as yet un-quantified shear stresses. When the balloon moves away from the endothelium, during deflation, it will generate micro pressure differences that may impose stretching (pulling) stresses on the ECs. Very high spatial resolution is required fully to interpret these effects at the cellular level. Such micro-scale information is also important in evaluating the performance of vascular stents, which very effectively dilate a stenosed artery to restore flow but at the near-wall micro-scale their constituent struts (side/diameter~100μm) apply stresses to the

endothelium and glycocalyx, disturbing local flow, causing further interaction with endothelial topography. Macroscopic models, like those of Raedelli et al. capture key flow details but cannot resolve crucial cellular and sub-cellular length-scales (36). The interaction of (portions of) a stent with individual blood cells, ECs and/or the glycocalyx is too demanding for conventional CFD.

Arguments of self-consistency, alone, require any model which resolves individual ECs also to resolve the cellular structure of blood. Furthermore, we have already commented, in section 2, on the unreliability, at the cellular micro-scale, of the concept of steady WSS. But the CFD analyses described in this section treat blood flow as the flow of a continuous fluid and represent the vascular endothelium as a constant, locally smooth velocity (Dirichlet) boundary condition. In reality, the vessel walls encounter Newtonian plasma, which advects discrete, particles which encounter the vessel wall in different ways, according to local flow conditions, geometry and cell concentration.

5 Multi-scale, multi-physics modeling

Human physiological systems subsume molecular and cellular, biological and physical processes, coupling the latter across orders of magnitude. For the problem of the interaction of explicitly resolved blood flow and the vessel wall, mediated by the vascular endothelium, the multi-scale modeling paradigm is effectively defined in the scale separation map (SSM) of Figure 5. There, the system is resolved into a closed set of *coupled,* single-scale models, or sub-systems, each mapped according to its characteristic spatial and temporal scales. Evans et al. (37) have shown how this analysis is developed for in-stent restenosis, in the coronary artery (see also www.complex-automata.org, (38) and Liu et al. diagrammatically depict, more qualitatively, key multiple-scale phenomena occurring in the cardio-vascular system (39). In fact, the SSM exemplar of figure 5 is not, in practice, definitive. The placement of and degree of resolution used in each sub-system reflects the extent of the modeled domain and the availability of quantitative data; the need to close the model requires one recursively to apply the multi-scale approach.

We have, in sections 3 and 4, shown that retaining short length and time scale fluctuations in WSS (which are a consequence of the mesoscopic constitution of blood) and the cellular structure of vascular endothelium are central to any self-consistent and properly founded understanding of atherosclerosis. It is, therefore, essential that a multi-scale model be founded, insofar as flow is concerned, on a simulation technique which is able efficiently to handle many advected Lagrangian particles (erythrocytes), to accommodate geometrically complex boundary conditions (see below) and multi-physical effects and (eventually) to facilitate multi-component flow extensions (to model leukocyte attachment). The overall demands of the problem suggest a need for parallelizable algorithms. Lattice Boltzmann equation (40) method (LBE) is a meso-scale technique which answers all these needs (appropriately optimised, it has been shown be able to simulate complex flow systems of comparable complexity on widely available computational platforms (41,42)). Figure 6 shows an instantaneous WSS distribution, over the boundary of a rectangular cross-section duct, at Re = 10, from a pressure-driven, suspension flow of spherical “erythrocytes”, at hematocrit concentration (40%), at what would be (in the continuum hemodynamic approximation) the steady state. Clearly, the spatial distribution of the WSS component $\eta\partial_y u_x$ reflects the distribution of particles immediately above the boundary. In the data of figure 6, the micro-scale effect of the glycocalyx has been represented simply by adding to the rigid spheres (each of radius 6 lattice units), and to the duct surfaces, a surface exclusion region with has an effect analogous to that of a lubrication force. A more sophisticated, meso-scale representation of glycocalyx effects would be inconsistent with the simplicity of the smooth boundary representation used for figure 6 (which clearly lacks any reference to the conformation of the EC layer). To simulate this flow in a completely self-consistent manner requires the use of agent based models (ABMs), which may be readily “two-way coupled” to flow

modalities- when the latter are computed using LBE.

ABMs have been successfully applied to problems similar to ours, defined in figure 5 (43,44). (Strictly, figure 5 refers to a complex cellular automata (CA) model, in which each component is a CA, in which the ABM is a single component representing smooth muscle cell migration and proliferation.) A software agent is an intuitive computational representation of a real world entity applicable to any system where emergent behaviour results from complex interactions between many individuals. Vascular endothelial behavior is an emergent property of the responses and interactions of individual ECs, individually represented by simple logical rule sets which determine the responses of individual software agents to biological and physical stimuli alike. Applying ABMs to endothelial tissue resolves the heterogeneity of individual ECs- each EC is permitted to react differently, depending on its gene/protein expression and differences in the local flow field. Sub-models of signaling processes, coupled to flow, extend the logical rule sets, adding further scales/complexity to the model.

6 Conclusion Currently, complex simulation chains which facilitate CFD analyses of models, developed from patient-specific geometries, are capable of providing information which, because of the limitations of current investigative techniques (in terms of resolution or the need for direct visualisation, by microscopic imaging of fluorescent particles, for example), is not available from clinical studies or experiment. The ultimate aim is to produce systems which couple haemodynamics with models of biological phenomena, at multiple scales, to test hypotheses or predict disease/intervention outcomes; the potential power of such models is now recognised.

We have argued that a closed multi-scale model of atherosclerotic initiation must capture interactions between representative numbers of explicitly modelled erythrocytes, endothelial cells and Newtonian plasma. Figure 6 clearly demonstrates the dangers inherent in the continuum haemodynamic approximation and points-out a need explicitly to resolve spatial and temporal fluctuations of wall shear stress. Figure 6 also demonstrates that the lattice Boltzmann equation method is, essentially, able to provide such data.

We have pointed-out that, to complete such a multi-scale model of atherosclerotic initiation, there is a clear need to model ingress of such atherosclerotic precursors such as leukocytes, which occurs at exposed endothelial cell boundaries. Implicitly, it is therefore necessary to impose geometrically complex, Dirichlet, boundary conditions, corresponding to the conformation of endothelial cells. The evolution of this boundary, we have argued is governed by wall shear stress and species mass transport (convection-diffusion), in processes located at meso-scales. This evolution of the endothelial state can feasibly be controlled by coupled agent-based models, predicated on the micro-scale. But micro-scale information, must also be coupled-into the model.

Future progress of our method depends on eg. course-grained molecular dynamic studies of emergent meso-scale effects of the cellular glycocalyx “layer”. No imaginable computer can resolve cellular-scale flow modalities and (albeit course-grained) molecular scales. Hence, the only means of incorporating into the critical meso-scale description, (see figures 5, 6) the influence of the glycocalyx is by modelling data from micro-scale studies, to find an effective boundary condition (6).

Several exciting initiatives are poised to accelerate progress and uptake of multi-scale modelling. Recognising the potential of ICT-based tools for simulation of human physiology and disease-related processes, the EU is funding collaborative projects directed towards the development of patient-specific computer models for personalised and predictive healthcare, under the banner of the *Virtual Physiological Human* (45). A networking action (the VPH Network of Excellence) within the recent European FP7 funding call attempts found methodological, technical and training frameworks to support research.

7 References

1. Libby P. Nature 2002; 420 (6917) pp868.

2. Cunningham K.S., Gotlieb AI. Lab Investig. (2005) 85 (1) pp9.
3. Bonetti, P. O., Lerman, L. O., and Lerman, A. (2003) Arterioscler Thromb Vasc Biol 23(2), pp168.
4. Caro, C. G., Fitz-Gerald, J. M., and Schroter, R. C. (1971) Proc R Soc Lond B Biol Sci 177(46), pp109
5. Ridger, V., Krams, R., Carpi, A. and Evans, P. C., Biomedicine and Pharmacotherapy 62 (2008) pp536.
6. Spencer, T. J., Hollis, A. P., Halliday, I. and Care, C. M., Proc. Brunel Conference (2009)
7. Ley K, Allietta M, Bullard DC, Morgan S., Circ Res (1998) 83(3) pp287.
8. Simon S.I., Hu Y., Vestweber D., Smith C.W., J. Immunol. (2000) 164(8) pp4348-58.
9. Sato, M., Ohshima, N., and Nerem, R. M. (1996) J Biomech 29(4), pp461.
10. Barbee, K. A., Davies, P. F., and Lal, R. (1994) Circ Res 74(1), pp163.
11. Helmlinger, G., Geiger, R. V., Schreck, S., and Nerem, R. M. (1991) J Biomech Eng 113(2), pp123.
12. Levesque, M. J., Liepsch, D., Moravec, S., and Nerem, R. M. (1986) Arteriosclerosis 6(2), pp220
13. Levesque, M. J., and Nerem, R. M., (1985) J Biomech Eng 107(4), pp341
14. Malek, A. M., Alper, S. L., and Izumo, S., (1999) Journal of the American Medical Association 282(21), pp2035
15. Chien, S., (2007) Am J Physiol Heart Circ Physiol 292(3), H pp1209.
16. Owatverot, T. B., Oswald, S. J., Chen, Y., Wille, J. J. and Yin, F. C., (2005) J Biomech Eng 127(3), pp374
17. Korenaga, R., Ando, J., Tsuboi, H., Yang, W., Sakuma, I., Toyo-oka, T., and Kamiya, A. (1994) Biochem Biophys Res Commun 198(1), pp213.
18. Malek, A., and Izumo, S., (1992) Am J Physiol 263(2 Pt 1), C pp389.
19. Levick, J. R. (2003) *An introduction to cardiovascular physiology*, Arnold, London.
20.Carlier, S. G., van Damme, L. C. A., Blommerde, C. P., Wentzel, J. J., van Langehove, G., Verheye, S., Kockx, M. M., Knaapen, M. W. M., Cheng, C., Gijsen, F., Duncker, D. J., Stergiopulos, N., Slager, C. J., Serruys, P. W., and Krams, R. (2003) Circulation 107(21), pp2741.
21. Ku, D. N., Giddens, D. P., Zarins, C. K., and Glagov, S. (1985) Arteriosclerosis 5(3), pp293.
22. LaMack, J. A., Himburg, H. A., Li, X. M., and Friedman, M. H. (2005) Ann Biomed Eng 33(4), pp457
23. Tardy, Y., Resnick, N., Nagel, T., Gimbrone, M. A., Jr., and Dewey, C. F., Jr. (1997) Arterioscler Thromb Vasc Biol 17(11), pp3102.
24. White, C. R., Haidekker, M., Bao, X., and Frangos, J. A. (2001) Circulation 103(20), 2508-2513
25. Demer, L. L., Wortham, C. M., Dirksen, E. R., and Sanderson, M. J. (1993) Am J Physiol 264(6 Pt 2), H pp2094.
26.Weinbaum, S., Tarbell, J. M., and Damiano, E. R. (2007) Annu Rev Biomed Eng 9, pp121.
27. Xu, X. Y., and Collins, M. W. (1990) Proc Inst Mech Eng [H] 204(4), pp205
28. Moravec, S., and Liepsch, D. (1983) Biorheology 20(6), pp745
29. Collins, M. W. and Xu, X. Y. (1990) *A predictive scheme for flow in arterial bifurcations: comparison with laboratory measurements*. In: al., F. M. e. (ed). *Biomechanical Transport Processes* Plenum Press.
30. Xu, X. Y., Collins, M. W., and Jones, C. J. (1992) J Biomech Eng 114(4), pp504.
31. Long, Q., Xu, X. Y., Collins, M. W., Griffith, T. M., and Bourne, M. (1998) Crit Rev Biomed Eng 26(4), pp227.
32. Xu, X. Y., Collins, M. W., and Jones, C. J. H. (1997) Adv. Eng. Softw. 28(6), pp365.
33. Roberts, J. C. J., Moses, C., and Wilkins, R. H. (1959) Circulation 20(4), pp511.
34. Jeays, A. D., Lawford, P. V., Gillott, R., Spencer, P., Barber, D. C., Bardhan, K. D., and Hose, D. R. (2007) J Biomech 40(9), pp1916.
35. DePaola, N., Gimbrone, M. A., Jr., Davies, P. F., and Dewey, C. F., Jr. (1992) Arterioscler Thromb 12(11), pp1254.
36. Radaelli, A. G., Sola, T., Vivas, E., Mellado, X., Guimaraens, L., Cebral, J. R., and Frangi, A. F. (2007) *Combined clinical*

and computational information in complex cerebral aneurysms: application to mirror cerebral aneurysms. In: Manduca, A., and Hu, X. P. (eds). Proc. SPIE Medical Imaging 2007: *Physiology, function, and structure from medical images*.
37. Evans, D. J. W., Lawford, P. V., Gunn, J., Walker, D., Hose, D. R., Smallwood, R. H., Chopard, B., Krafczyk, M., Bernsdorf, J., and Hoekstra, A. G. (2008) Philosophical Transactions of the Royal Society A. In Press.
38. Hoekstra, A., Lorenz, E., Falcone, J., and Chopard, B. (2007) International Journal for Multiscale Computational Engineering 5, pp491.
39. Liu, W. K. et al. Comput. Methods Appl. Mech. Engrg. 195 (2006) pp1722.
40. Succi, S. *The Lattice Boltzmann Equation for Fluid Mechanics and Beyond*, Oxford.
41. Lishchuk, S. V., Halliday, I. and Care, C. M., Phys Rev E 74 017701 (2006)
42. Dupin, M. M., Munn, L., Halliday, I., and Care, C. M., Phys. Rev. E 75, 066707 (2007)
43. Walker, D. C., Hill, G., Wood, S. M., Smallwood, R. H., and Southgate, J. (2004) Ieee Transactions on Nanobioscience 3(3), 153-163
44. Walker, D. C., Southgate, J., Hill, G., Holcombe, M., Hose, D. R., Wood, S. M., Mac Neil, S., and Smallwood, R. H. (2004) Biosystems 76(1-3), 89-100
45.http://www.biomedtown.org/biomed_town/STEP/Reception/step-efinitions/VirtualPhysiologicalHuman

8 Figure Captions

Figure 1 Major components of a healthy artery showing the three wall layers (intima, media and adventitia) and the distribution of endothelial and smooth muscle cells.

Figure 2 **a** The mechanical environment of the artery showing the distribution of wall stresses **b.** The influence of shear stress on endothelial cell morphology.

Figure 3 Subject-specific CFD model of the abdominal aorta and the superior mesenteric artery (SMA). **a** OSI distribution. The region of high OSI (arrowed) at the proximal lip of the outlet of the origin of the SMA from the aorta corresponds with the normal distribution of atheroma reported for this artery. **b** plots of the different time varying WSS at two locations on the vessel wall. One corresponds to an area of high OSI (top), the second to an area of low OSI (bottom).

Figure 4 Evolution of the wall shear stress spatial gradient [Pa/m] for an idealised aneurysm with a localized daughter bleb developing on the dome. Development of the aneurysm is accompanied by an increase in the WSSG around its base: this may have significant implications for the degenerative remodeling of the tissue in this region and thus future growth of the aneurysm. At /t/=10, a daughter bleb begins to develop on the aneurysm dome. It can be seen that an annulus of high WSSG forms around the daughter bleb (/t/=12). This may result in further degeneration of the tissue in this region thus promoting the growth and enlargement (and possibly rupture) of the secondary bleb.

Figure 5 A scale Separation Map (SSM) is a two dimensional map with the horizontal (vertical) axis coding for temporal (spatial) scales. A subsystem occupies a certain area on this map. Arrows indicate coupling between the single scale sub-systems.

Figure 6 The fiction of steady WSS. The magnitude of instantaneous WSS component $\eta\partial_y u_x$ plotted over one plane boundary of a rectangular cross-section duct, obtained, for a flowing suspension of softened, rigid spheres (see text) at normal haematocrit concentration (40%), *Re* = 10, at the "steady state" of continuum haemodynamics. The flow is pressure driven. The complex WSS distribution reflects the positions of particles immediately above the boundary.

9 Figures

Figure 1

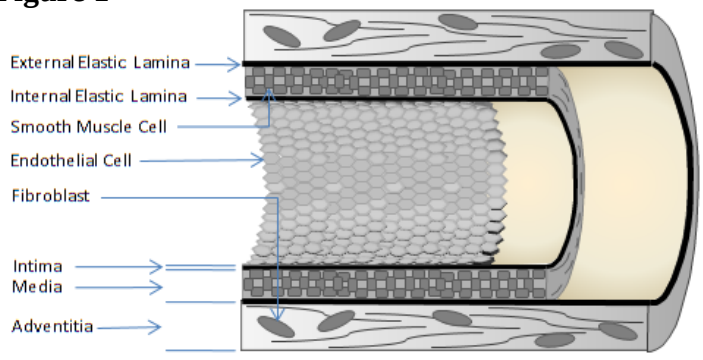

Figure 2 a / b

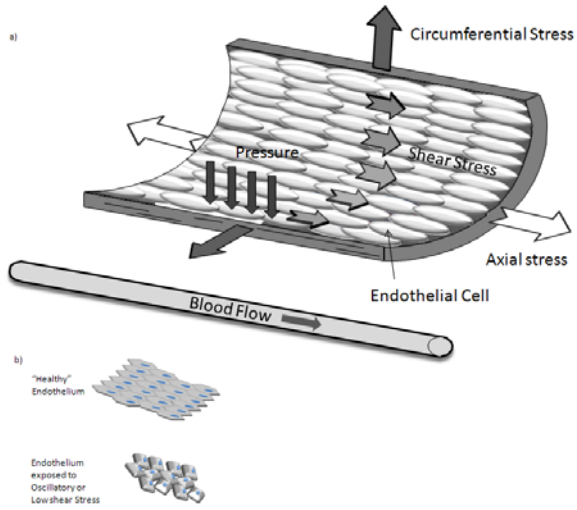

Figure 3

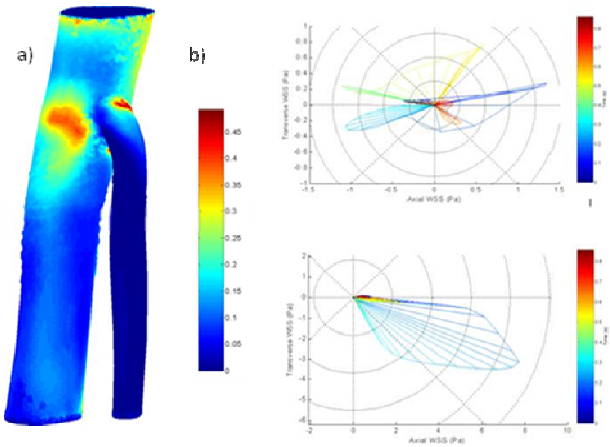

Figure 4

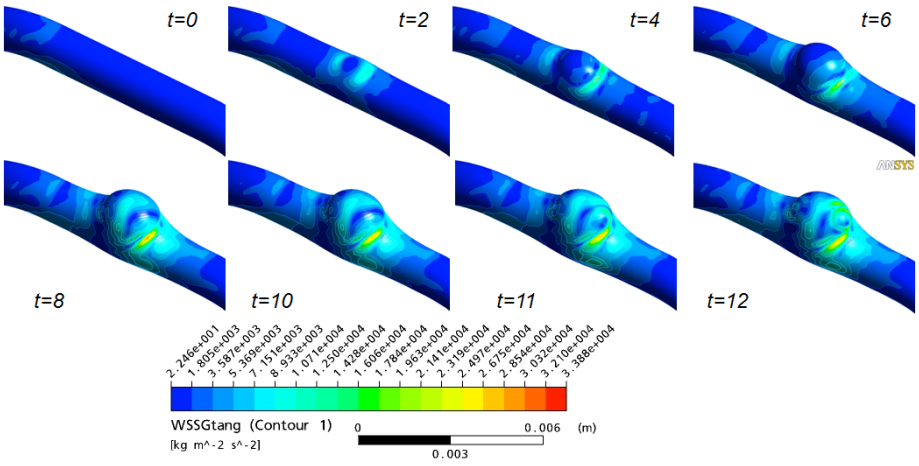

Figure 5

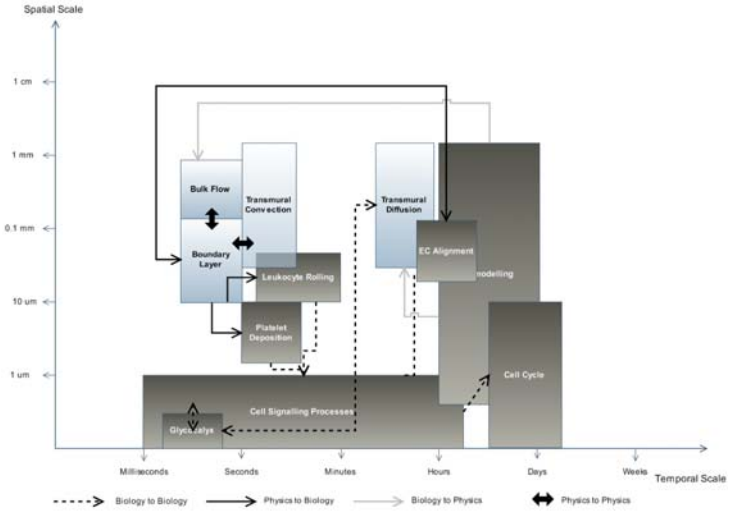
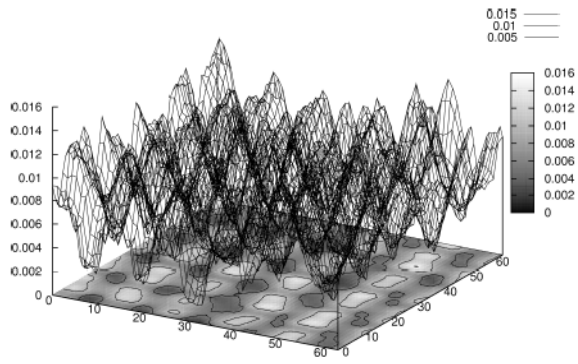
Figure 6